

## Neural-Network Approach to Dissipative Quantum Many-Body Dynamics

Michael J. Hartmann<sup>1,2,3</sup> and Giuseppe Carleo<sup>4</sup>

<sup>1</sup>*Institute of Photonics and Quantum Sciences, Heriot-Watt University Edinburgh EH14 4AS, United Kingdom*

<sup>2</sup>*Google Research, Erika-Mann-Str. 33, 80636 München, Germany*

<sup>3</sup>*Department of Physics, University of Erlangen-Nürnberg (FAU), 91058 Erlangen, Germany*

<sup>4</sup>*Center for Computational Quantum Physics, Flatiron Institute, 162 5th Avenue, New York, New York 10010, USA*



(Received 28 February 2019; published 28 June 2019)

In experimentally realistic situations, quantum systems are never perfectly isolated and the coupling to their environment needs to be taken into account. Often, the effect of the environment can be well approximated by a Markovian master equation. However, solving this master equation for quantum many-body systems becomes exceedingly hard due to the high dimension of the Hilbert space. Here we present an approach to the effective simulation of the dynamics of open quantum many-body systems based on machine-learning techniques. We represent the mixed many-body quantum states with neural networks in the form of restricted Boltzmann machines and derive a variational Monte Carlo algorithm for their time evolution and stationary states. We document the accuracy of the approach with numerical examples for a dissipative spin lattice system.

DOI: [10.1103/PhysRevLett.122.250502](https://doi.org/10.1103/PhysRevLett.122.250502)

The description of interacting quantum many-body systems presents a formidable challenge for theoretical and numerical approaches. A pure many-body quantum state is described by the wave function, whose complexity grows exponentially with the number of constituents. This challenge is even more pronounced for mixed quantum states, where the fundamental object describing all physical properties is the density matrix, whose number of degrees of freedom scales quadratically with the dimension of the Hilbert space [1]. Yet the description of experiments under realistic conditions requires modeling in terms of density matrices as the systems of interest are never perfectly isolated from their environment. The huge number of degrees of freedom of pure and mixed states, however, renders an exact description of large systems in general infeasible (see [2,3] for exceptions with exact solutions), even if one resorts to numerical approaches.

To meet this quantum complexity challenge, several approximate approaches have been developed. Tensor networks and the density matrix renormalization group [4,5] become efficient descriptions whenever the amount of entanglement contained in the modeled states is restricted. Despite substantial effort [6], these methods however still suffer from limitations in systems with more than one lattice dimension. For two-dimensional systems, novel real-space renormalization-based approaches are among the most promising existing tools [7], although their application to large systems is at present at the forefront of research activity [8]. Stochastic many-body techniques, such as quantum Monte Carlo (QMC) methods [9,10], rely on sampling a number of physically relevant configurations or perform an efficient compression of the quantum state. However, QMC

approaches are effective only for a restricted number of open quantum systems and regimes [11,12], and a severe sign problem typically emerges in the simulation of dissipative dynamics.

Recently, machine-learning inspired approaches and parametrizations of wave functions in terms of neural networks have been introduced [13]. This variational representation, dubbed neural-network quantum states (NQS), has been used to study both system at equilibrium [13–17], and out of equilibrium, in the context of unitary dynamics of pure states [18–20]. The connection between NQS and tensor network representations has also been explored [15,21,22]. While in the past years there have been several methodological developments to study open quantum systems using tensor network representations [23–30], the description of mixed states with NQS has been so-far explored for data-driven tomographic purposes [31–33].

For modeling quantum experiments, particularly for open many-body systems [34–38], there is a strong need for efficient and accurate approaches, especially in more than one lattice dimension, where tensor networks face difficulties. To this end, it is instrumental to develop a flexible and scalable numerical approach to study mixed state dynamics or stationary states of dissipative dynamics. Central to this goal is the ability to use variational density-matrix states not facing the entanglement problem, and flexible enough to describe correlations and many-body effects beyond mean-field [39,40] and cluster approaches [41,42].

Here we present a machine-learning approach to the simulation of dissipative quantum dynamics and its stationary states. Our approach uses a neural-network parametrization for the quantum density matrix [31] and a

stochastic learning method to approximate its dynamics in a time-dependent variational Monte Carlo approach [43]. Our approach is suitable to model nonunitary dynamics of quantum systems with many degrees of freedom in a variety of settings. These include numerical characterizations of near term quantum computers where decoherence processes due to their imperfections are taken into account [44]. A second field of applications is the investigation of stationary state quantum phases and phase transitions, which have attracted increasing interest in recent years [34–38,45,46].

*Problem and parametrization.*—Our aim is to solve the quantum master equation of Lindblad form,

$$\dot{\rho} = -i[H, \rho] + \sum_j \frac{\gamma_j}{2} (2c_j \rho c_j^\dagger - c_j^\dagger c_j \rho - \rho c_j^\dagger c_j), \quad (1)$$

where  $\rho$  is the density matrix of the system,  $H$  its Hamiltonian, and the  $\gamma_j$  and  $c_j$  the dissipation rates and jump operators of its dissipation. The index  $j$  runs over all dissipation channels. For a large class of models, there is however only one dissipation channel per lattice site and we restrict our treatment to this case, where  $j$  thus labels the lattice sites. As an example, we consider a dissipative and anisotropic Heisenberg model for a lattice of  $N$  spin-1/2 degrees of freedom that has attracted significant interest recently [41].

To find an efficient and accurate approximation to the dynamics of Eq. (1), we leverage the idea that artificial neural networks can be used to provide compact representations of quantum states [13]. Specifically, we use a parametrization of the density matrix in terms of complex-valued restricted Boltzmann machines (RBM), similar to the one introduced in Ref. [31]. Figure 1 shows a sketch of the specific neural-network architecture used in this work. It most prominently features three sets of hidden units,  $h^{(l)}$ ,  $h^{(r)}$  and  $h^{(m)}$ , whose role is to mediate correlations among, respectively, column degrees of freedom of the density

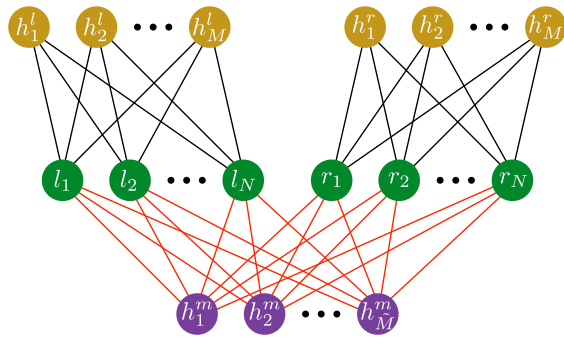


FIG. 1. Sketch of the employed neural network. The visible layer is in green and hidden layers are in light brown and purple. There is a hidden layer for the row indices  $l_i$  and the column indices  $r_i$  of  $\rho$  ( $i = 1, 2, \dots, N$ ) with hidden neurons  $h_j^l$  and  $h_j^r$  ( $j = 1, \dots, M$ ). A further hidden layer with neurons  $h_k^m$  ( $k = 1, \dots, \tilde{M}$ ) is responsible for the mixing, cf., [31].

matrix, row degrees of freedom, and mixed correlations between the two. Because of the bipartite structure of the RBM interactions, the hidden units can be integrated out exactly, resulting in a parametrization that guarantees a Hermitian and positive semidefinite density matrix [31],

$$\begin{aligned} \rho_{\vec{l}, \vec{r}} &= \exp \left[ \sum_{j=1}^N (a_j l_j + a_j^* r_j) \right] \prod_{k=1}^M \mathcal{X}_k \prod_{p=1}^{\tilde{M}} \mathcal{Y}_p \\ \mathcal{X}_k &= \cosh \left( b_k + \sum_{j=1}^N W_{k,j} l_j \right) \cosh \left( b_k^* + \sum_{j=1}^N W_{k,j}^* r_j \right) \\ \mathcal{Y}_p &= \cosh \left( c_p + c_p^* + \sum_{j=1}^N (U_{p,j} l_j + U_{p,j}^* r_j) \right), \end{aligned} \quad (2)$$

where the vector indices  $\vec{l} = (l_1, l_2, \dots)$  and  $\vec{r} = (r_1, r_2, \dots)$  contain the left (right) indices  $l_j$  ( $r_j$ ) for all lattice sites  $j$ , and the variational parameters are the complex-valued weights  $W_{k,j}$ ,  $U_{p,j}$  and biases  $a_j$ ,  $b_k$  and  $c_p$ . Analogously to the pure state case, increasing the number of hidden units,  $M$  and  $\tilde{M}$ , guarantees more expressive representations of the density matrix. Given the RBM parametrization of the density matrix, it remains to be determined how to find an approximate solution of the Lindblad master equation. The approximation of the dynamics generated by Eq. (1) can be recast as a variational optimization problem that can be approached via a suitable extension of the stochastic reconfiguration method [47] and the time-dependent variational Monte Carlo [43] to the dissipative case.

*Stochastic reconfiguration for Liouvillians.*—It is convenient to write the density matrix  $\rho$  as a vector  $\vec{\rho}$  such that the right-hand side of Eq. (1) can be expressed as the action of a linear operator on  $\vec{\rho}$ , i.e.,  $\partial_t \vec{\rho} = \mathcal{L} \vec{\rho}$ , where  $\mathcal{L}$  is the Liouvillian superoperator that, in contrast to the Hamiltonian  $H$ , is not Hermitian.

According to Eq. (2), the density matrix  $\vec{\rho}$  is parametrized by a set of  $(N+1)(M+\tilde{M})+N$  complex variational parameters. In the following, we use the abbreviate notation  $\vec{\alpha}$  to indicate the ensemble of these variational parameters. Most notably, the real vector  $\vec{\alpha}$  contains both imaginary and real parts of the variational parameters that are treated independently. The time derivative of the variational  $\rho$  can in turn be expressed in terms of the time derivative of the variational parameters as

$$\partial_t \vec{\rho} = \sum_k \dot{\alpha}_k O_k \vec{\rho}, \quad (3)$$

where  $O_k$  denote diagonal matrices whose nonzero matrix elements read  $[O_k]_{\vec{l}, \vec{r}; \vec{l}, \vec{r}} = \partial \ln(\rho_{\vec{l}, \vec{r}}) / (\partial \alpha_k)$ . To get the best approximation to the dynamics of the density matrix, our goal is to find a closed equation of motion for the variational parameters, namely, the time dependence  $\alpha(t)$ . To this end, at each instant in time we consider the difference between the exact Lindblad infinitesimal time evolution and the approximate variational evolution,

$$\delta = \left\| \sum_k \dot{\alpha}_k O_k \vec{\rho} - \vec{\mathcal{L}} \vec{\rho} \right\|_2^2, \quad (4)$$

where the time derivatives of the variational parameters,  $\dot{\alpha}_k$ , are to be determined. Minimization of  $\delta$  with respect to  $\dot{\alpha}_k$  leads to the system of equations

$$\sum_p S_{k,p} \dot{\alpha}_p = f_k, \quad (5)$$

where

$$S_{k,p} = \vec{\rho}^\dagger O_k^\dagger O_p \vec{\rho} + \vec{\rho}^\dagger O_p^\dagger O_k \vec{\rho}, \quad (6)$$

$$f_k = \vec{\rho}^\dagger O_k^\dagger \vec{\mathcal{L}} \vec{\rho} + \vec{\rho}^\dagger \vec{\mathcal{L}}^\dagger O_k \vec{\rho}, \quad (7)$$

and it is easy to show that the solutions of Eq. (5) are indeed local minima of  $\delta$ ; see Supplemental Material [48]. Alternatively to the 2-norm in Eq. (4), one can also use the Fubini-Study norm; see Supplemental Material [48]. Equation (5) can be written as a first order differential equation,

$$\partial_t \vec{\alpha} = \mathcal{S}^{-1} \vec{f}, \quad (8)$$

where  $S_{k,p}$  are the matrix elements of the matrix  $\mathcal{S}$  and  $f_k$  the elements of the vector  $\vec{f}$ .

*Stochastic sampling.*—The expressions in Eqs. (6) and (7) cannot be exactly computed for systems with a large number of quantum particles. However, those quantum expectations can be conveniently interpreted as statistical expectation values over the probability distribution

$$p(\vec{l}, \vec{r}) = |\rho_{\vec{l}, \vec{r}}|^2, \quad (9)$$

in analogy to the concept in static and time-dependent variational Monte Carlo. The elements of  $\mathcal{S}$  and  $\vec{f}$  can thus also be written as

$$S_{k,p} \propto \text{Re} \langle O_k^\dagger O_p \rangle_p \quad \text{and} \quad f_k \propto \text{Re} \langle O_k^\dagger \mathcal{L}^{\text{res}} \rangle_p, \quad (10)$$

where  $\langle \dots \rangle_p$  denotes a statistical expectation value of the probability distribution  $p$  as in Eq. (9), and we have introduced the following estimator for the Liouvillian,

$$\mathcal{L}_{\vec{l}_1, \vec{r}_1; \vec{l}_2, \vec{r}_2}^{\text{res}} = \sum_{\vec{l}_2, \vec{r}_2} \frac{\mathcal{L}_{\vec{l}_1, \vec{r}_1; \vec{l}_2, \vec{r}_2} \rho_{\vec{l}_2, \vec{r}_2}}{\rho_{\vec{l}_1, \vec{r}_1}}. \quad (11)$$

In addition to having a stochastic strategy for solving the variational equations of motion, it is also important to provide an efficient scheme to compute expectation values of physical observables. Consider the expectation value of a generic observable  $X$ ,

$$\langle X \rangle = \text{Tr} \{ X \rho \} = \sum_{\vec{l}, \vec{m}} X_{\vec{l}, \vec{m}} \rho_{\vec{m}, \vec{l}}. \quad (12)$$

Estimates of  $\langle X \rangle$  can be obtained in this case as statistical averages over the probability distribution  $q(\vec{l}) = \rho_{\vec{l}, \vec{l}}$ , such that

$$\langle X \rangle \simeq \langle X^{\text{loc}} \rangle_q, \quad X_{\vec{l}, \vec{l}}^{\text{loc}} = \sum_{\vec{m}} \frac{X_{\vec{l}, \vec{m}} \rho_{\vec{m}, \vec{l}}}{\rho_{\vec{l}, \vec{l}}}. \quad (13)$$

In all cases of physical relevance, observables  $X$  have a sparse representation, and computing the estimator  $X_{\vec{l}, \vec{l}}^{\text{loc}}$  can be efficiently realized. Notice that, while possible, sampling over  $p(\vec{l}, \vec{m})$  to compute physical expectation values would entail a much less efficient statistical estimator for  $\langle X \rangle$ . This would further require one to stochastically estimate the normalization factor, which is instead automatically taken into account when sampling from  $q(\vec{l})$ . In this work we use two independent Markov-chain Monte Carlo schemes to obtain samples both from  $p(\vec{l}, \vec{r})$  and from  $q(\vec{l})$  at each instant of time, as explained in the Supplemental Material [48].

*Results.*—To test the accuracy of our method, we consider an anisotropic Heisenberg model with Hamiltonian

$$H = \sum_{j=1}^N B \sigma_j^z + \sum_{\langle j, l \rangle} \sum_{a=x, y, z} J_a \sigma_j^a \sigma_l^a, \quad (14)$$

where  $\sum_{\langle j, l \rangle}$  denotes the sum over all nearest neighbors, and dissipator

$$\mathcal{D}[\rho] = \frac{\gamma}{2} \sum_{j=1}^N (2\sigma_j^- \rho \sigma_j^+ - \sigma_j^+ \sigma_j^- \rho - \rho \sigma_j^+ \sigma_j^-). \quad (15)$$

Whereas our method can be applied equally to one- and two-dimensional lattices, we here present examples for one-dimensional lattices where we can compare the results to matrix product state (MPS) simulations. We consider two applications. First we compare the time evolution of a density matrix as obtained from Eq. (8) to the exact time evolution of the density matrix for a small size model where the full master equation (1) can be numerically integrated. Then we show that our method correctly finds stationary states for a larger model that can no longer be fully integrated but where a MPS representation of  $\rho$  [49] allows one to find the stationary state.

To quantify the accuracy of a time evolution for  $\rho$  as obtained from Eq. (8), we consider two quantities. (i) The average deviation of the matrix element of  $\rho$  from the exact density matrix  $\rho^e$  is given by

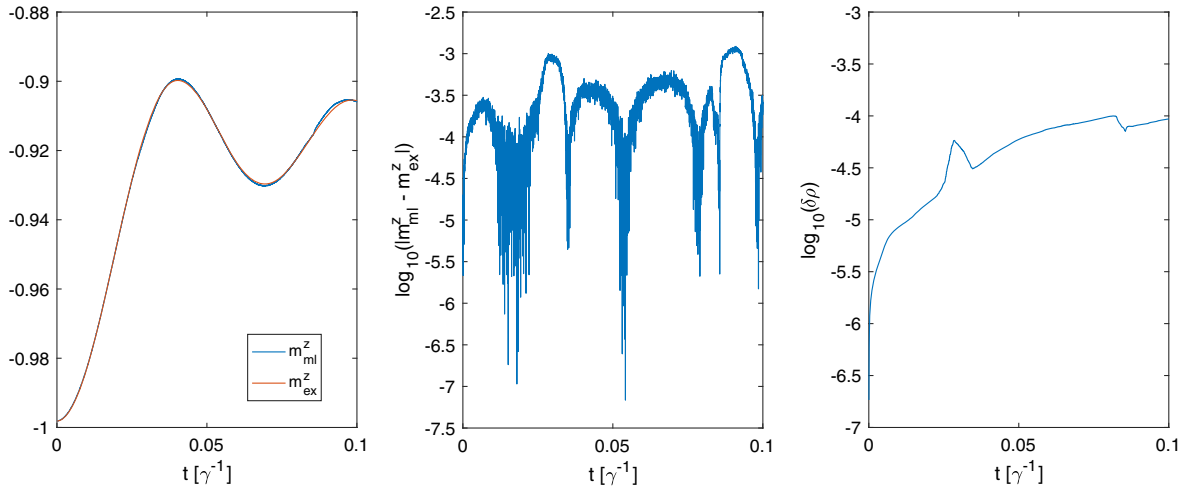


FIG. 2. Results for a chain of five spins with periodic boundary conditions and  $B = 10\gamma$ ,  $J_x = 20\gamma$ ,  $J_y = 0$ , and  $J_z = 10\gamma$ .  $M = \tilde{M} = 20$ , the sample size was  $N_S = 10^6$ , and the time step of fourth order Runge-Kutta integration was  $\delta t = 2 \times 10^{-5}\gamma^{-1}$ . (a) Magnetization for the neural-network approximation,  $\langle \sigma^z \rangle$  (blue) and the exact solution,  $\langle \sigma^z \rangle_e$  (orange). (b) Log plot of difference between  $\langle \sigma^z \rangle$  and  $\langle \sigma^z \rangle_e$ . (c) Average deviation of the matrix element of  $\rho$  from the exact density matrix  $\rho_e$  as given by Eq. (16).

$$\delta\rho = \frac{1}{2^{2N}} \sum_{j,l} |\rho_{j,l} - \rho_{j,l}^e|^2 = \frac{\|\rho - \rho^e\|_2^2}{2^{2N}}, \quad (16)$$

where  $\|x\|$  is the 2-norm of a matrix  $x$ . (ii) To get an accuracy test in terms of physical observables we compare the magnetization for our approximation

$$m_{ml}^z = \frac{1}{N} \sum_j \langle \sigma_j^z \rangle \quad (17)$$

to the magnetization for an exact solution  $m_{ex}^z = (1/N) \sum_j \langle \sigma_j^z \rangle_{\text{exact}}$ .

Results for a linear chain with  $N = 5$  spins and periodic boundary conditions are presented in Fig. 2 and clearly show that the parametrization of the density matrix  $\rho$  in terms of the neural network in Fig. 1 provides a very good approximation to the dissipative quantum dynamics of mixed states.

To show that our method correctly finds stationary states for models where the full density matrix can no longer be computed, we test whether  $\mathcal{L}\rho = 0$ . To this end we compute

$$\delta\mathcal{L} = \langle |\mathcal{L}^{\text{res}}| \rangle_p. \quad (18)$$

Since  $\delta\mathcal{L} = \sum_{\vec{l}_1, \vec{r}_1} |\rho_{\vec{l}_1, \vec{r}_1}| |(\mathcal{L}\rho)_{\vec{l}_1, \vec{r}_1}|$  this tests whether all matrix elements  $(\mathcal{L}\rho)_{\vec{l}_1, \vec{r}_1}$  vanish. Moreover, the measure  $\delta\mathcal{L}$  weights the matrix elements of  $\mathcal{L}\rho$  according to the relevance for the state  $\rho$  and is very economic to compute.  $\delta\mathcal{L}$  can thus be computed as a test for the convergence to the stationary state, even if the properties of the latter are completely unknown. Notice that since  $\delta\mathcal{L}$  can be efficiently estimated (as well as other related quantities such as  $|\mathcal{L}\rho|^2 \propto \langle |\mathcal{L}^{\text{res}}|^2 \rangle_p$ , at the same cost of applying  $\mathcal{L}$  once, it

is, in principle, possible to devise an alternative variational optimization scheme that directly minimizes  $\delta\mathcal{L}$ , if only the stationary state is of interest.

In addition to computing  $\delta\mathcal{L}$ , we also test whether the magnetization, see Eq. (17), approaches the steady state magnetization  $m_{SS}^z = \lim_{t \rightarrow \infty} (1/N) \sum_j \langle \sigma_j^z \rangle$ , which we obtain from an integration with a MPS representation of the density matrix  $\rho$ . Results for the approach to the stationary state of a chain with  $N = 16$  spins and open boundary conditions are presented in Fig. 3 and show that the stationary state is found with high accuracy. For finding stationary states, we make use of the fact that the parametrization (2) always guarantees a physically valid state.

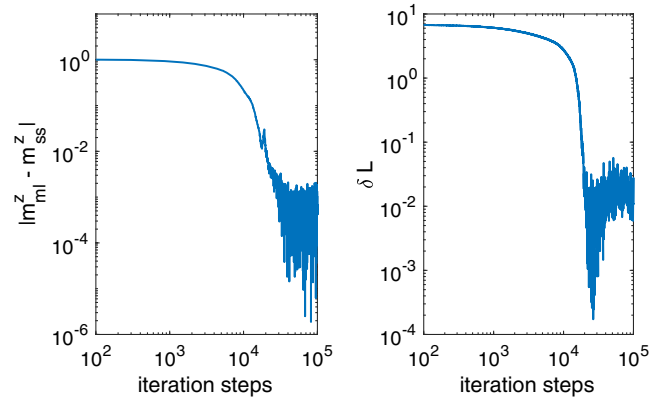


FIG. 3. Results for a chain of 16 spins with open boundary conditions  $B = 10\gamma$ ,  $J_x = \gamma$ ,  $J_y = 0$ , and  $J_z = 0$ .  $M = \tilde{M} = 12$ , the sample size was  $N_S = 2 \times 10^5$ , and a second order Runge-Kutta integration with adaptive step size was used. (a) Difference between  $m_{ml}^z$ , see Eq. (17), and  $m_{SS}^z = -15.9286$  as found from an integration with MPS, and (b) magnitude of  $\mathcal{L}\rho$  as quantified by  $\delta\mathcal{L}$  given in Eq. (18).

If we do not aim at correctly modeling the dynamics for all times, we can thus choose the integration time step larger and still find convergence to the correct stationary state.

The example presented here features a moderately correlated state where a MPS representation of the steady state with bond dimension  $D = 17$  suffices to compute  $m_{SS}^z$  with an accuracy of  $10^{-4}$ . Hence, the MPS representation here requires  $4[(N - 2)D^2 + 2D] = 16320$  parameters (the prefactor 4 is the physical dimension for mixed states of spin systems), whereas the neural-network representation achieves a comparable approximation with only  $(N + 1)(M + \tilde{M}) + N = 424$  parameters. Scenarios with stronger spin-spin interactions would require more variational parameters and larger sample sizes, increasing the numerical effort of the method.

*Conclusions.*—We have introduced a neural-network-based approach to numerically modeling the quantum dynamics and stationary quantum states of open or dissipative quantum many-body systems. Our results show that both the dynamics and stationary states of such systems can be obtained with high accuracy. In this work we have shown one-dimensional systems, in order to provide benchmarks with existing approaches. Several extensions of our approach can be envisaged for future research. From the point of view of applications, the study of two-dimensional lattices does not present conceptual difficulties, and represents an interesting opportunity for our method. From the methodological point of view, schemes targeting only the stationary state can also be efficiently implemented, using the same ideas introduced to compute  $\delta\mathcal{L}$  in this work.

M. J. H. thanks Heriot-Watt University for support. We acknowledge stimulating discussions with V. Savona, C. Ciuti, F. Vicentini, and G. Torlai.

*Note added.*—Recently, Refs. [50–52] appeared, which discuss similar strategies to study stationary states of open quantum many-body systems by using complex-valued neural networks.

---

[1] H.-P. Breuer, *The Theory of Open Quantum Systems* (Oxford University Press, Oxford, USA, 2007).  
 [2] T. Prosen, Exact Nonequilibrium Steady State of a Strongly Driven Open  $xxz$  Chain, *Phys. Rev. Lett.* **107**, 137201 (2011).  
 [3] T. Prosen, Exact Nonequilibrium Steady State of an Open Hubbard Chain, *Phys. Rev. Lett.* **112**, 030603 (2014).  
 [4] U. Schollwöck, The density-matrix renormalization group in the age of matrix product states, *Ann. Phys. (Amsterdam)* **326**, 96 (2011).  
 [5] F. Verstraete, V. Murg, and J. I. Cirac, Matrix product states, projected entangled pair states, and variational renormalization group methods for quantum spin systems, *Adv. Phys.* **57**, 143 (2008).

[6] A. Kshetrimayum, H. Weimer, and R. Orús, A simple tensor network algorithm for two-dimensional steady states, *Nat. Commun.* **8**, 1291 (2017).  
 [7] S. Finazzi, A. Le Boité, F. Storme, A. Baksic, and C. Ciuti, Corner-Space Renormalization Method for Driven-Dissipative Two-Dimensional Correlated Systems, *Phys. Rev. Lett.* **115**, 080604 (2015).  
 [8] R. Rota, F. Minganti, C. Ciuti, and V. Savona, Quantum Critical Regime in a Quadratically-Driven Nonlinear Photonic Lattice, *Phys. Rev. Lett.* **122**, 110405 (2019).  
 [9] D. Ceperley and B. Alder, Quantum Monte Carlo, *Science* **231**, 555 (1986).  
 [10] W. M. C. Foulkes, L. Mitás, R. J. Needs, and G. Rajagopal, Quantum Monte Carlo simulations of solids, *Rev. Mod. Phys.* **73**, 33 (2001).  
 [11] Z. Yan, L. Pollet, J. Lou, X. Wang, Y. Chen, and Z. Cai, Interacting lattice systems with quantum dissipation: A quantum Monte Carlo study, *Phys. Rev. B* **97**, 035148 (2018).  
 [12] A. Nagy and V. Savona, Driven-dissipative quantum Monte Carlo method for open quantum systems, *Phys. Rev. A* **97**, 052129 (2018).  
 [13] G. Carleo and M. Troyer, Solving the quantum many-body problem with artificial neural networks, *Science* **355**, 602 (2017).  
 [14] D.-L. Deng, X. Li, and S. Das Sarma, Machine learning topological states, *Phys. Rev. B* **96**, 195145 (2017).  
 [15] I. Glasser, N. Pancotti, M. August, I. D. Rodriguez, and J. Ignacio Cirac, Neural-Network Quantum States, String-Bond States, and Chiral Topological States, *Phys. Rev. X* **8**, 011006 (2018).  
 [16] R. Kaubruegger, L. Pastori, and J. C. Budich, Chiral topological phases from artificial neural networks, *Phys. Rev. B* **97**, 195136 (2018).  
 [17] K. Choo, G. Carleo, N. Regnault, and T. Neupert, Symmetries and Many-Body Excitations with Neural-Network Quantum States, *Phys. Rev. Lett.* **121**, 167204 (2018).  
 [18] M. Schmitt and M. Heyl, Quantum dynamics in transverse-field Ising models from classical networks, *SciPost Phys.* **4**, 013 (2018).  
 [19] S. Czischek, M. Gärttner, and T. Gasenzer, Quenches near Ising quantum criticality as a challenge for artificial neural networks, *Phys. Rev. B* **98**, 024311 (2018).  
 [20] B. Jónsson, B. Bauer, and G. Carleo, Neural-network states for the classical simulation of quantum computing, [arXiv:1808.05232](https://arxiv.org/abs/1808.05232).  
 [21] J. Chen, S. Cheng, H. Xie, L. Wang, and T. Xiang, Equivalence of restricted Boltzmann machines and tensor network states, *Phys. Rev. B* **97**, 085104 (2018).  
 [22] L. Pastori, R. Kaubruegger, and J. C. Budich, Generalized transfer matrix states from artificial neural networks, *Phys. Rev. B* **99**, 165123 (2019).  
 [23] F. Verstraete, J. J. García-Ripoll, and J. I. Cirac, Matrix Product Density Operators: Simulation of Finite-Temperature and Dissipative Systems, *Phys. Rev. Lett.* **93**, 207204 (2004).  
 [24] M. Zwolak and G. Vidal, Mixed-State Dynamics in One-Dimensional Quantum Lattice Systems: A Time-Dependent Superoperator Renormalization Algorithm, *Phys. Rev. Lett.* **93**, 207205 (2004).

- [25] R. Orús and G. Vidal, Infinite time-evolving block decimation algorithm beyond unitary evolution, *Phys. Rev. B* **78**, 155117 (2008).
- [26] J. Cui, J. Ignacio Cirac, and M. Carmen Bañuls, Variational Matrix Product Operators for the Steady State of Dissipative Quantum Systems, *Phys. Rev. Lett.* **114**, 220601 (2015).
- [27] E. Mascarenhas, H. Flayac, and V. Savona, Matrix-product-operator approach to the nonequilibrium steady state of driven-dissipative quantum arrays, *Phys. Rev. A* **92**, 022116 (2015).
- [28] A. H. Werner, D. Jaschke, P. Silvi, M. Kliesch, T. Calarco, J. Eisert, and S. Montangero, Positive Tensor Network Approach for Simulating Open Quantum Many-Body Systems, *Phys. Rev. Lett.* **116**, 237201 (2016).
- [29] A. A. Gangat, T. I, and Y.-J. Kao, Steady States of Infinite-Size Dissipative Quantum Chains via Imaginary Time Evolution, *Phys. Rev. Lett.* **119**, 010501 (2017).
- [30] D. Jaschke, S. Montangero, and L. D. Carr, One-dimensional many-body entangled open quantum systems with tensor network methods, *Quantum Sci. Technol.* **4**, 013001 (2018).
- [31] G. Torlai and R. G. Melko, Latent Space Purification via Neural Density Operators, *Phys. Rev. Lett.* **120**, 240503 (2018).
- [32] J. Carrasquilla, G. Torlai, R. G. Melko, and L. Aolita, Reconstructing quantum states with generative models, *Nat. Mach. Intell.* **1**, 155 (2019).
- [33] L. Banchi, E. Grant, A. Rocchetto, and S. Severini, Modelling nonMarkovian quantum processes with recurrent neural networks, *New J. Phys.* **20**, 123030 (2018).
- [34] S. Diehl, A. Micheli, A. Kantian, B. Kraus, H. P. Büchler, and P. Zoller, Quantum states and phases in driven open quantum systems with cold atoms, *Nat. Phys.* **4**, 878 (2008).
- [35] J. T. Barreiro, M. Müller, P. Schindler, D. Nigg, T. Monz, M. Chwalla, M. Hennrich, C. F. Roos, P. Zoller, and R. Blatt, An open-system quantum simulator with trapped ions, *Nature (London)* **470**, 486 (2011).
- [36] M. Fitzpatrick, N. M. Sundaresan, A. C. Y. Li, J. Koch, and A. A. Houck, Observation of a Dissipative Phase Transition in a One-Dimensional Circuit QED Lattice, *Phys. Rev. X* **7**, 011016 (2017).
- [37] M. C. Collodo, A. Potočnik, S. Gasparinetti, J.-C. Besse, M. Pechal, M. Sameti, M. J. Hartmann, A. Wallraff, and C. Eichler, Observation of the Crossover from Photon Ordering to Delocalization in Tunably Coupled Resonators, *Phys. Rev. Lett.* **122**, 183601 (2019).
- [38] R. Ma, B. Saxberg, C. Owens, N. Leung, Y. Lu, J. Simon, and D. I. Schuster, A dissipatively stabilized Mott insulator of photons, *Nature (London)* **566**, 51 (2019).
- [39] J. Marino and S. Diehl, Quantum dynamical field theory for nonequilibrium phase transitions in driven open systems, *Phys. Rev. B* **94**, 085150 (2016).
- [40] W. Casteels, R. M. Wilson, and M. Wouters, Gutzwiller Monte Carlo approach for a critical dissipative spin model, *Phys. Rev. A* **97**, 062107 (2018).
- [41] J. Jin, A. Biella, O. Viyuela, L. Mazza, J. Keeling, R. Fazio, and D. Rossini, Cluster Mean-Field Approach to the Steady-State Phase Diagram of Dissipative Spin Systems, *Phys. Rev. X* **6**, 031011 (2016).
- [42] A. Biella, J. Jin, O. Viyuela, C. Ciuti, R. Fazio, and D. Rossini, Linked cluster expansions for open quantum systems on a lattice, *Phys. Rev. B* **97**, 035103 (2018).
- [43] G. Carleo, F. Becca, M. Schiro, and M. Fabrizio, Localization and glassy dynamics of many-body quantum systems, *Sci. Rep.* **2**, 243 (2012).
- [44] J. Preskill, Quantum computing in the NISQ era and beyond, *Quantum* **2**, 79 (2018).
- [45] E. M. Kessler, G. Giedke, A. Imamoglu, S. F. Yelin, M. D. Lukin, and J. I. Cirac, Dissipative phase transition in a central spin system, *Phys. Rev. A* **86**, 012116 (2012).
- [46] M. J. Hartmann, Quantum simulation with interacting photons, *J. Opt.* **18**, 104005 (2016).
- [47] S. Sorella, M. Casula, and D. Rocca, Weak binding between two aromatic rings: Feeling the van der Waals attraction by quantum Monte Carlo methods, *J. Chem. Phys.* **127**, 014105 (2007).
- [48] See Supplemental Material at <http://link.aps.org/supplemental/10.1103/PhysRevLett.122.250502> for details of the derivations and algorithm.
- [49] M. J. Hartmann, Polariton Crystallization in Driven Arrays of Lossy Nonlinear Resonators, *Phys. Rev. Lett.* **104**, 113601 (2010).
- [50] N. Yoshioka and R. Hamazaki, Constructing neural stationary states for open quantum many-body systems, *Phys. Rev. B*, **99**, 214306 (2019).
- [51] F. Vicentini, A. Biella, N. Regnault, and C. Ciuti, following Letter, Variational Neural Network Ansatz for Steady States in Open Quantum Systems, *Phys. Rev. Lett.* **122**, 250503 (2019).
- [52] A. Nagy and V. Savona, preceding Letter, Variational Quantum Monte Carlo with Neural Network Ansatz for Open Quantum Systems, *Phys. Rev. Lett.* **122**, 250501 (2019).